THE CHEMICAL COMPOSITIONS AND TEXTURES OF MATRICES AND CHONDRULE RIMS OF EIGHT UNEQUILIBRATED ORDINARY CHONDRITES: A PRELIMINARY REPORT

Satoshi MATSUNAMI

Geological Institute, Faculty of Science, University of Tokyo, 3–1, Hongo 7-chome, Bunkyo-ku, Tokyo 113

Abstract: The matrices and chondrule rims of eight unequilibrated ordinary chondrites, Semarkona (LL3), Krymka (L3), Sharps (H3), Chainpur (LL3), Tieschitz (H3), Mezö-Madaras (L3), ALH-77214 (L3) and ALH-77216 (L3), have been investigated in detail with the scanning electron microscope. The analyses were made by the SEM-EDS technique, using a Link System Model 860 energy dispersive spectrometer equipped to a JEOL-T200.

Although chondrule rims have similarities in texture and composition to matrices, chondrule rims show wider variabilities in chemical composition in comparison with matrices and often have significantly different compositions from the matrices. From compositional relationships between matrix and rim materials and chondrules in Semarkona, it is shown that the most non-refractory, FeO-rich chondrule rims might have been one of the non-refractory components of precursor materials of the Semarkona chondrules, suggesting that chondrules and and matrix and rim materials have one common component in Semarkona.

1. Introduction

The fine-grained matrix material (often opaque in thin section) surrounding chondrules in unequilibrated ordinary chondrites (UOCs) has long been considered to be the primitive substance such as low-temperature condensates from the primitive solar nebula gas (*e.g.*, WOOD, 1963; ANDERS, 1964; LARIMER and ANDERS, 1967, 1970; GROSSMAN and LARIMER, 1974). Recently, chondrule rims surrounding chondrules in UOCs have attracted much attention (ALLEN *et al.*, 1980; ASHWORTH, 1977; KING and KING, 1981). Although the major chemical compositions of matrices and chondrule rims in UOCs have been published (*e.g.*, HUSS *et al.*, 1981; IKEDA *et al.*, 1981; ALLEN *et al.*, 1980), comparative studies of chemical compositions between matrices and chondrule rims are particularly scarce. This study was made to provide detailed data on chemical compositions and textures of matrices and chondrule rims in UOCs, to clarify the differences in composition and texture among chondrules, matrices and chondrule rims, and to discuss the compositional relationships among them.

2. Method of Investigations

Polished thin sections of eight type 3 ordinary chondrites (Table 1) were studied microscopically under transmitted and reflected light. Textures of matrices and chondrule-rim materials of all the specimen were studied in detail by scanning electron microscope (SEM), JEOL-T200.

Table 1. List and classification of ordinary chondrites studied.

Meteorite	Sample No.	Type	Source of chips and polished thin section
ALH-77214		L3	NIPR (chip)
ALH-77216		L3	NIPR (chip)
Chainpur	USNM 1251	LL3	Smithson. Inst. (chip)
Krymka	USNM 2488	L3	Smithson. Inst. (chip)
Mezö-Madaras	USNM 4838-3	L3	Smithson. Inst. (pts)
Semarkona	USNM 1805	LL3	Smithson. Inst. (chip)
Sharps		H3	Smithson. Inst. (chip)
Tieschitz	USNM 3093-2	H3	Smithson. Inst. (pts)

The SEM-EDS analyses of the matrices and chondrule rims in UOCs were made, using a Link System Model 860 energy-dispersive spectrometer, equipped to a JEOL-T200 (SEM). The accelerating voltage is 15 kV and the specimen current is 3×10^{-9} A. Counting time is 100 s for each analysis. Bulk chemical compositions of matrices and chondrule rims were determined by scanning an area of approximately (10–30 μm)^2. The apparent weight percent of oxides was obtained by ZAF correction method. The S content of matrices was determined as S_2O. The C content was not determined. During the SEM-EDS analyses of matrix materials, particles of metal, troilite and magnetite were avoided to obtain chemical compositions of silicate portion of fine-grained matrix materials.

FeS and metallic Ni-Fe were calculated on the basis of measured S_2O and NiO contents by the modified method of a normative procedure (Lux *et al.*, 1980; Huss *et al.*, 1981). First, S and Ni were subtracted from the apparent total oxide weight % combined with the amounts of Fe to form troilite (FeS) and metallic Ni-Fe, assuming that all S is in FeS and all Ni is in Ni-Fe metal containing 8 wt% Ni for H chondrites, 13 % Ni for L chondrites, and 20 % for LL chondrites. These compositions are based on the average Ni/Fe ratio of the meteorite's chemical groups (Keil, 1969). Next, the weight percent of the remaining FeO and other oxides was recalculated to 100 as bulk chemical composition of silicate portions of matrix materials. Obviously this procedure is not rigorously correct, but yields analyses with enough accuracy to compare these analyses with each other.

In order to check the accuracy of SEM-EDS analyses, one powdered (grain size <20 μm) mixture composed of fayalitic olivine (60 wt%), bronzite (20 wt%) and albite glass (20 wt%) was prepared and pressed into pellet at 1050°C and 18 kb during 15 min. The pellet roughly simulates the matrix materials of UOCs in composition and texture (porosity and surface roughness). It was polished and analyzed by the SEM-EDS technique. Calculated bulk chemical composition from analytical data of olivine, bronzite and albite and the obtained analytical bulk chemical composition of the mixture are shown in Table 2. The analyzed bulk composition well agrees with the calculated composition, except for MgO which is 1.4 wt% lower than that of calculated value. Relatively large error in MgO is unaccountable. Similar uncertainty for the MgO content was also reported for the broad beam analyses in wave-dispersive system by Huss *et al.* (1981).

Table 2. Comparison of SEM-EDS analyses (20 areas averaged) of a polished pellet, which is powdered mixtures made of Fa-rich olivine, bronzite and albite glass (powder grain size <20 μm), to the calculated analyses (in wt %; normalized to total 100%).

	1	2	3
SiO_2	43.3	43.6	+.3
TiO_2	.00	.06	+.06
Al_2O_3	3.91	4.51	+.60
Cr_2O_3	.01	.11	+.10
FeO*	36.2	36.0	−.2
MnO	2.38	2.01	−.37
MgO	11.4	10.0	−1.4
CaO	.32	.44	+.12
Na_2O	2.25	2.82	+.57
K_2O	.00	.06	+.06
P_2O_5	.00	.03	+.03
Total	99.77	99.64	

1: Calculated bulk composition; 2: Broad area analysis;
3: (Analyzed)-(Calculated); *: All iron reported as FeO.

3. Texture of Matrix Materials

3.1. Terminology

In this study, as already mentioned by many investigators, the author distinguishes two modes of occurrence of fine-grained materials in UOCs; matrix and chondrule rim. These two modes are easily distinguished under microscope and/or SEM.

What is generally called "matrix" in UOCs is usually defined as the fine-grained dark material filling interstitial spaces between chondrules, fragment of chondrules and particles of silicate, Ni-Fe metals and troilite under microscope (ALLEN *et al.*, 1980; HUSS *et al.*, 1981). To avoid the ambiguity in the definition of "matrix", IKEDA *et al.* (1981) proposed to define the matrix of UOCs as aggregates of materials finer than micron-size. But these definitions might include chondrule rims by default (ALLEN *et al.*, 1980). In this study, to compare the chemical compositions of matrices and chondrule rims, chondrule rims were distinguished from matrix and mineral fragments as carefully as possible, based on clear textural differences under the SEM observation. In most cases, the contact boundary of the chondrule rim and matrix is well defined in meteorite samples studied here. In this paper, therefore, modifying the definition of matrix by IKEDA *et al.* (1981), the matrix of UOCs is tentatively defined as aggregates composed mostly of micron- to submicron-sized grains, which can be clearly recognized not to be chondrule-rimming materials under SEM, excluding crystal grains larger than a few microns.

3.2. Petrographical observations

In the following paragraphs, the author briefly describes observed textural features of the fine-grained materials in chondrite samples studied.

3.2.1 Textural features of matrices and chondrule rims

Most of the opaque matrices of meteorite samples (Semarkona, Krymka, Sharps,

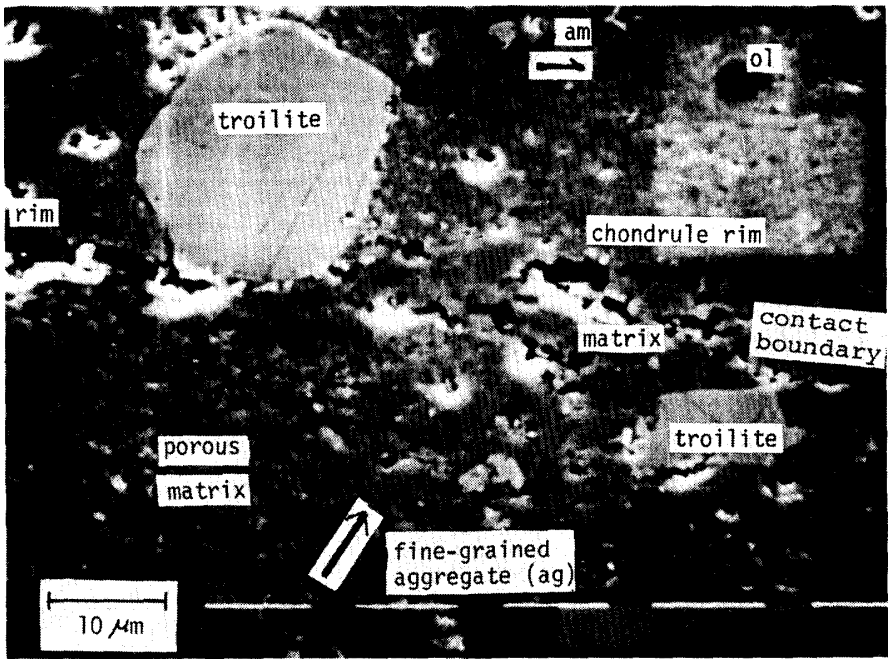

Fig. 1. SEM photograph of the boundary between fine-grained matrix and a chondrule rim of Semarkona, showing the clear boundary between them and the clastic texture consisting mainly of micron-sized, subround to subangular silicate crystals, possibly amorphous materials (am), aggregates of very fine-grained materials (ag) and minute grains of opaque minerals (troilite).

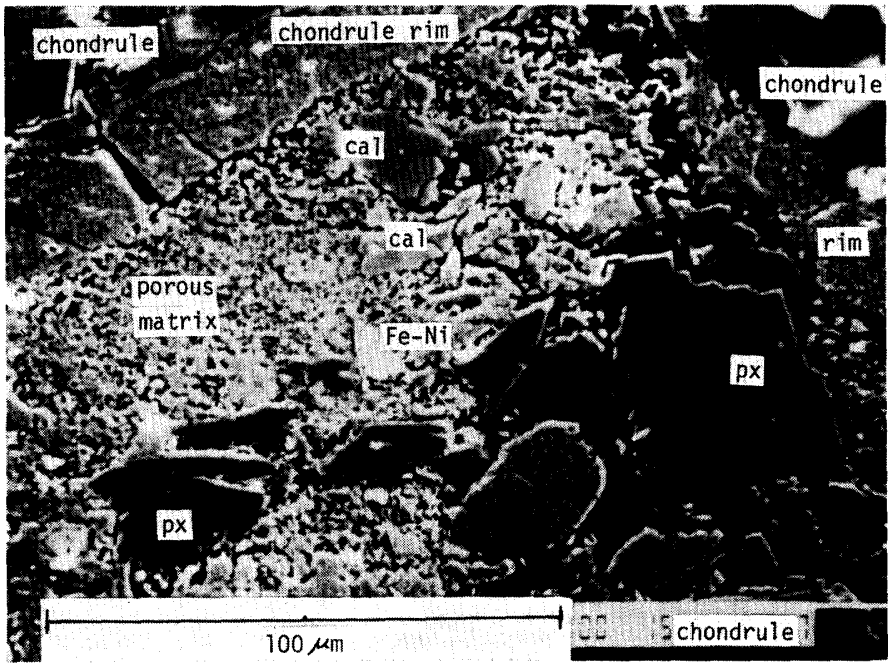

Fig. 2. SEM photograph of clastic matrix and chondrule rims of Semarkona, showing a typical relationship among chondrules, matrix and chondrule rims in Semarkona, characterized by high matrix/chondrule-rim ratio. The chondrule rims show less porous texture than the matrix, consisting of micron-sized silicate grains, pyroxene fragments (px), calcite grains (cal) and opaque minerals (Fe-Ni).

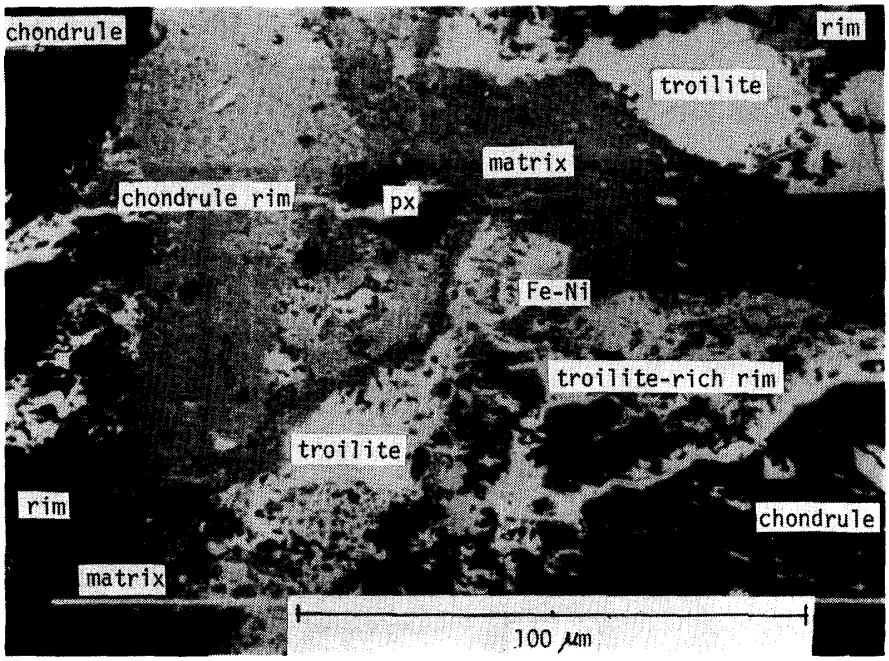

Fig. 3. SEM photograph of chondrule rims and matrix of Krymka, showing a typical relationship among chondrules, matrix and chondrule rims in Krymka, characterized by well-rimmed chondrules and low matrix/chondrule-rim ratio.

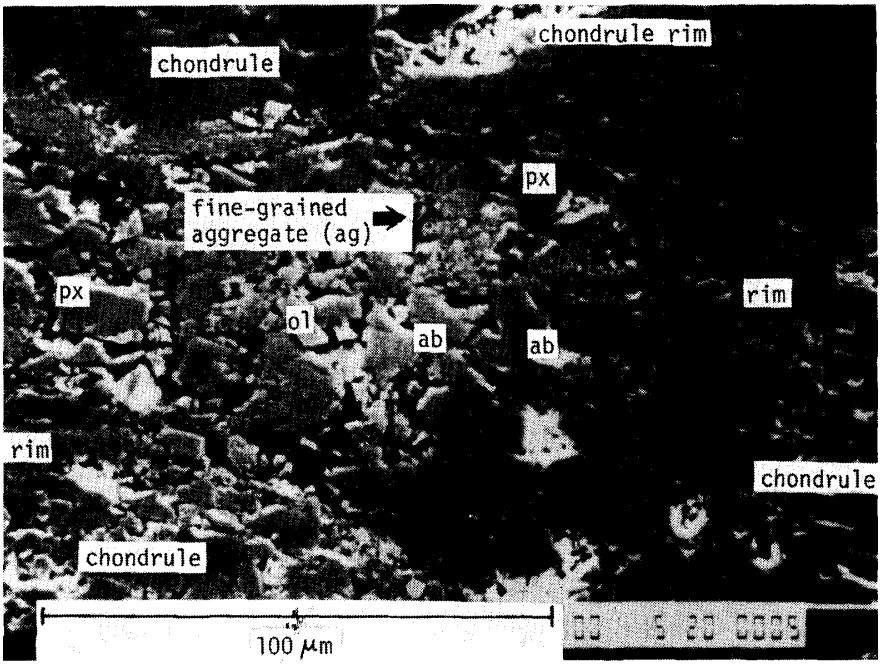

Fig. 4. SEM photograph of clastic matrix of Tieschitz, showing a porous texture consisting of olivine (ol), pyroxene (px), albite-like particles (ab) (NAGAHARA, 1984) and aggregates of micron-sized materials (ag).

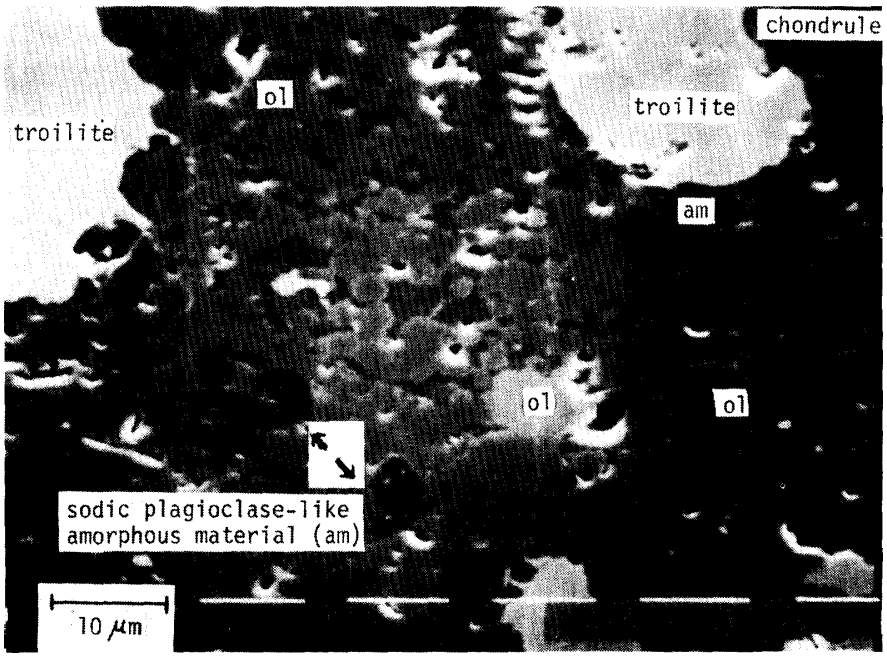

Fig. 5. SEM photograph of recrystallized matrix of ALH-77216, showing a coarse-grained, well-sintered and less porous texture compared with those in other samples, consisting of micron-sized olivine crystals (2–10 μm in diameter) (ol) and interstitial sodic plagioclase-like amorphous materials (am).

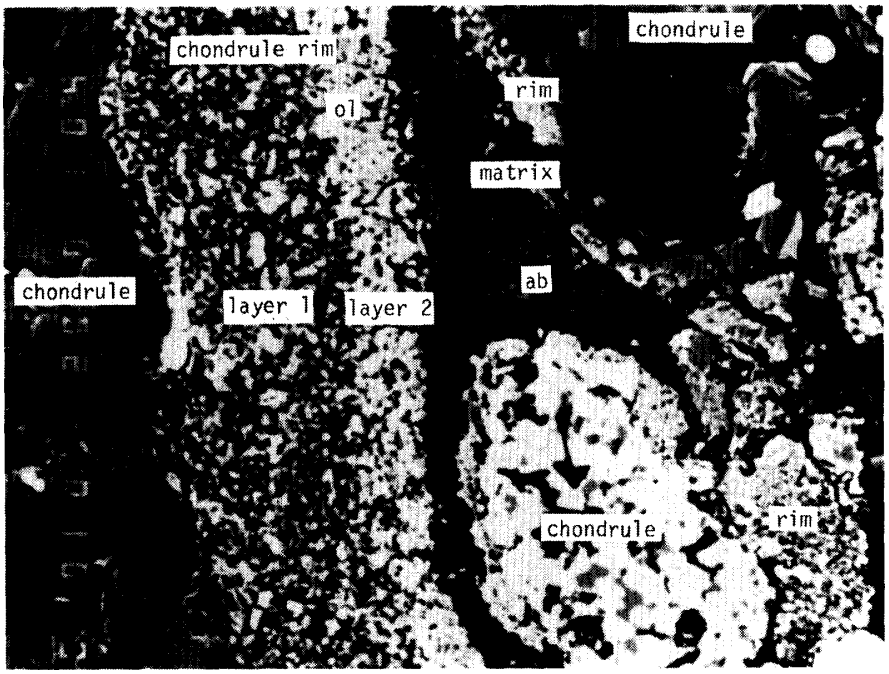

Fig. 6. SEM photograph of the internal structure of a chondrule rim in Tieschitz, showing a marked layered structure composed of two concentric layers, i.e., inner olivine-poor layer 1 and outer olivine-rich layer 2. Width 100 μm.

Chainpur, Mezö-Madaras and ALH-77214 chondrites) showsimilar textures and are found to consist predominantly of micron-sized, subround to subangular silicate crystals, possibly amorphous materials, aggregates of very fine-grained ($\sim$0.1 μm in diameter) materials (Fig. 1), and minute grains of troilite, metallic Ni-Fe and/or magnetite (HUSS *et al.*, 1981; NAGAHARA, 1984; MATSUNAMI, 1984). Interstitial spaces between these grains are sometimes filled by loose aggregates of possibly amorphous materials, which appear to connect these fine-grained materials to each other as "glue" (Fig. 1) (HUSS *et al.*, 1981; MATSUNAMI, 1984). Chondrule rims are commonly discontinuous and variable in thickness, and chondrules are often in contact with matrix materials directly. These chondrite samples are characterized by apparent high matrix/chondrule-rim ratio (Fig. 2). However, the Krymka chondrite is characterized by the closed packing of chondrules with well-developed rims, which commonly touch (Fig. 3). Krymka has a low matrix/chondrule-rim ratio. Porosity is apparently lower than that of other samples. In general, chondrule rims are well preserved and no fragmentation of chondrule rims is appreciable in Krymka.

On the other hand, the matrix of Tieschitz shows an especially porous texture (CHRISTOPHE MICHEL-LÉVY, 1976; NAGAHARA, 1984) (Fig. 4). The matrix includes what corresponds to the 'white matrix' of CHRISTOPHE MICHEL-LÉVY (1976). It is composed of fine-grained materials similar to those of the matrices in other samples and is poor in the connecting materials such as those in Semarkona. Interstitial spaces between large silicate grains remain usually open. The mean size of these silicate grains in the matrix of Tieshitz is apparently larger than those of the matrices in other samples. The relationships among chondrules, matrix and rims in Tieschitz are characterized by the well-packed arrangement of less rimmed chondrules and coarse-grained matrix (Fig. 4).

A portion of the matrix of ALH-77216 is sufficiently coarse-grained to recognize under microscope in thin section. This matrix is called coarse-grained or recrystallized matrix, following the difinition of HUSS *et al.* (1981). The matrix and chondrule rims are characterized by well-sintered, coarse-grained, less opaque, less friable and less porous appearance than those in the other chondrites studied in SEM images (Fig. 5). Coarse-grained nature may be attributable to grain growth of constituent grains due to metamorphism (ASHWORTH, 1977; HUSS *et al.*, 1981).

3.2.2. Thickness and internal structures of chondrule rims

The apparent thickness of chondrule rims is shown in Fig. 7, which is obtained from the SEM observation. The thickness of chondrule rims is ranging mainly from 5 to 40 μm. Rarely, very thick chondrule rims upto 100 μm are observed. A chondrule bearing such a thick rim might correspond to the so-called dark-zoned chondrule (DODD and VAN SCHMUS, 1971).

Although thickness of chondrule rims appears to be generally uniform, it is variable on some chondrules. The chondrule rims are not always continuous, and are occasionally broken, suggesting fragmentation of the chondrule rims prior to accretion of chondrules and matrices.

Several chondrule rims show marked layered structures composed of two or more concentric layers (ALLEN *et al.*, 1980; ASHWORTH, 1977). Two types of concentric rims are distinguished. One is characterized by the presence of inner silicate-rich layer and

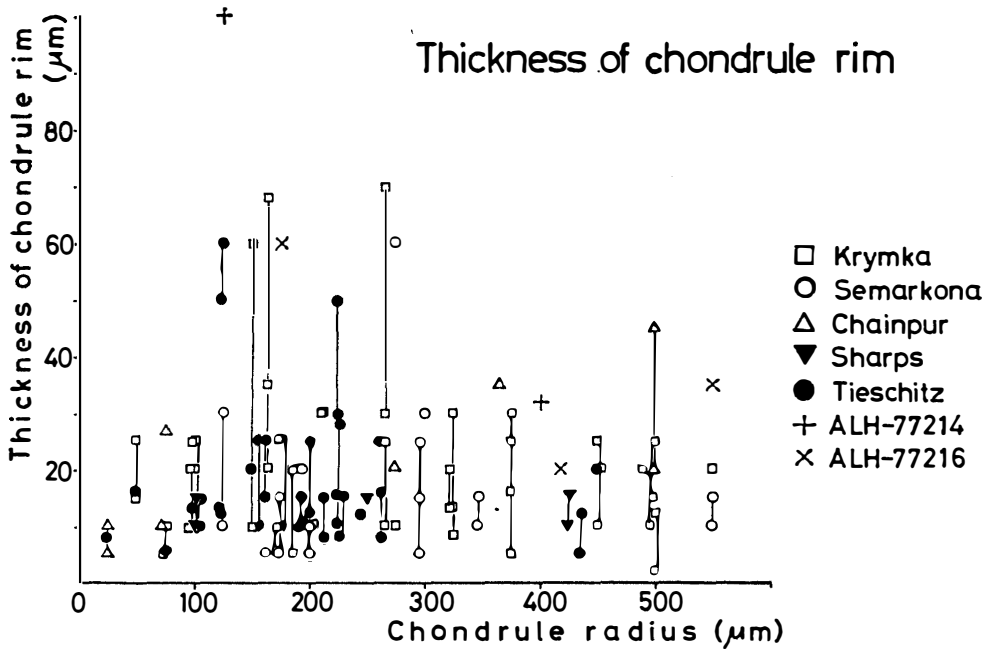

Fig. 7. Relations between apparent chondrule radius and thickness of chondrule rim. Bar represents the range of varying thickness of a chondrule rim.

outer another silicate-rich layer, which are easily distinguished by the different modal compositions of silicate grains. An example of Tieschitz is shown in Fig. 6. In the other type, troilite is concentrated in the outermost parts of the rim, and silicate grains are predominant in the inner part. Thus, the latter type is characterized by the inner silicate-rich layer and outer troilite-rich layer. These structures of chondrule rims are common in chondrule rims of the Krymka chondrite.

4. Analytical Results

Average SEM-EDS analyses for the bulk silicate portion of the matrix and chondrule rim of samples studied here, normalized to 100%, the CIPW norms, and the FeO/(FeO+MgO) mole ratios are tabulated in Table 3. Representative analyses are listed in Appendix. Furthermore, the SiO_2-oxides variation diagrams for Semarkona are shown in Fig. 8.

4.1. Major element chemistry

Fine-grained materials in UOCs show a broad continuum of compositions ranging from SiO_2 29 to 58 wt%. For matrices and rims, there is a marked inverse correlation of FeO with SiO_2, and relatively weak positive correlations of MgO, Al_2O_3, CaO, Na_2O and K_2O with SiO_2. Exceptionally, those of Tieschitz and ALH-77214 show weak negative correlations of MgO with SiO_2 (MATSUNAMI, 1984).

The matrix of Semarkona is characterized by high SiO_2 (42–51 wt%), high alkalis (Na_2O=2–4 wt%, K_2O=0.2–1.0 wt%), high Al_2O_3 (1.8–5.8 wt%) contents, which result in high normative plagioclase (19.4% in average) and hypersthene (33.9% in average) (Table 3 and Fig. 8). The rims show wider compositional ranges than those

Table 3. Average chemical compositions and the CIPW norms of matrices and chondrule rims of chondrite samples studied here, recalculated to total 100%, on a metallic Fe-Ni and troilite-free basis (N: the number of analytical areas averaged).

	Semarkona		Krymka		Sharps		Chainpur	
	matrix	chondrule rim	matrix	chondrule rim	matrix	chondrule rim	matrix	chondrule rim
N	27	28	13	40	14	7	19	14
SiO_2	47.7	42.8	35.4	38.3	37.8	38.7	36.5	36.4
TiO_2	.12	.09	.08	.12	.11	.10	.12	.09
Al_2O_3	3.73	3.38	2.80	3.77	2.73	3.53	1.86	1.62
Cr_2O_3	.45	.33	.33	.28	.30	.61	.44	.43
FeO	26.7	38.7	46.4	39.2	37.7	35.3	38.0	37.8
MnO	.30	.21	.48	.47	.61	.51	.55	.47
MgO	16.3	11.0	13.1	15.1	17.8	18.0	20.6	21.8
CaO	1.05	.76	.76	1.80	1.20	1.37	1.01	.55
Na_2O	2.84	2.03	.20	.48	1.02	1.38	.57	.55
K_2O	.55	.52	.13	.19	.35	.32	.06	.05
P_2O_5	.10	.09	.12	.14	.16	.03	.15	.10
C	0	0	1.22	0	0	0	0	0
or	3.22	3.04	.78	1.13	2.08	1.90	.36	.30
ab	16.17	14.51	1.71	4.02	7.63	9.17	4.83	4.66
an	0	0	2.97	7.53	1.82	2.49	2.35	1.81
ne	0	0	0	0	.56	1.33	0	0
di-wo	1.88	1.32	0	.23	1.28	1.70	.71	.14
en	.85	.39	0	.08	.50	.70	.30	.06
fs	1.02	.99	0	.15	.79	1.02	.41	.08
hy-en	15.36	5.70	3.50	4.83	0	0	.18	.08
fs	18.50	14.65	9.20	9.29	0	0	.25	.10
fo	17.19	15.10	20.45	23.01	30.84	30.86	35.69	38.03
fa	22.83	42.79	59.27	48.78	53.48	49.66	53.71	53.73
cm	.67	.49	.48	.42	.44	.90	.65	.63
il	.23	.17	.15	.23	.21	.19	.23	.17
ap	.24	.22	.29	.31	.38	.07	.36	.21
ns	1.84	.61	0	0	0	0	0	0
X_{Fe}	.48	.66	.67	.59	.54	.52	.51	.49
FeNi	.50	.58	.87	.91	.35	.31	.15	.22
FeS	.44	.40	.06	.28	.04	.05	.09	.04

of the matrices; SiO_2=29–51 wt%, Na_2O=0–3.5 wt%, K_2O=0–1.2 wt%, Al_2O_3=0.3–8.6 wt%. The SiO_2-poorest rims have the highest FeO contents (60-66 wt%). Most of SiO_2-richer rims have similar compositions to those of the matrices.

The matrix of Krymka is characterized by low SiO_2 (29–45 wt%), with an average of SiO_2=35 wt%, high FeO (26–60 wt%), low MgO (8–25 wt%), low alkalis (Na_2O=0–0.8 wt%; K_2O=0–0.4 wt%), and low CaO (0.2–2.4 wt%) contents. The rims show wider variations than the matrices (SiO_2=29–57 wt%, Al_2O_3=0.5–9.0 wt%, FeO=1–62 wt%, MgO=6–26 wt%, CaO=0–11.2 wt%, Na_2O=0–1.9 wt%).

The fine-grained materials of Sharps, Chainpur, ALH-77214 and Mezö-Madaras are also characterized by low SiO_2 contents, with average SiO_2 contents ranging from 36 to 41 wt%, low alkali contents (Na_2O=0.6–1.2 wt%, K_2O=0.1–0.35 wt% in average), and high normative ol contents ranging from 80 to 90 wt% (Table 3). The matrices

Table 3 (continued).

	Tieschitz		ALH-77214		Mezö-Madaras		ALH-77216	
	matrix	chondrule rim	matrix	chondrule rim	matrix	chondrule rim	matrix	chondrule rim
N	13	48	70	7	55	14	7	4
SiO_2	45.9	39.7	37.0	44.3	39.5	46.9	45.8	48.9
TiO_2	.15	.15	.12	.20	.13	.18	.13	.22
Al_2O_3	8.14	3.80	2.12	3.29	2.70	4.25	5.54	5.31
Cr_2O_3	.29	.40	.54	.58	.63	.66	.74	.47
FeO	21.9	31.7	32.3	22.8	25.5	15.9	17.5	14.4
MnO	.37	.52	.46	.52	.53	.54	.44	.26
MgO	15.1	19.4	25.5	21.9	28.0	25.4	24.4	23.0
CaO	2.02	1.52	.83	2.95	1.23	3.28	2.40	4.91
Na_2O	5.00	2.06	.61	1.89	1.17	2.03	2.20	1.66
K_2O	.33	.27	.10	.10	.15	.17	.29	.19
P_2O_5	.61	.32	.31	1.31	.30	.58	.37	.52
C	0	0	.23	0	0	0	0	0
or	1.96	1.62	.59	.59	.83	1.01	1.72	1.12
ab	27.70	11.94	4.17	16.00	7.80	17.28	18.66	14.06
an	0	.32	2.12	.19	1.70	1.94	4.35	6.49
ne	6.67	4.04	.55	0	1.12	0	0	0
di-wo	2.54	2.06	0	2.50	1.02	4.46	2.17	6.05
en	1.21	1.07	0	1.36	.58	2.85	1.34	3.88
fs	1.30	.99	0	1.05	.39	1.32	.71	1.77
hy-en	0	0	0	10.66	0	11.38	6.63	19.77
fs	0	0	0	8.21	0	5.28	3.50	9.03
fo	25.64	39.75	44.55	29.85	48.58	34.29	37.12	23.62
fa	30.33	36.86	46.05	25.34	36.12	17.55	21.61	11.89
cm	.43	.45	.80	.86	.92	.98	1.09	.69
il	.29	.21	.23	.38	.25	.34	.25	.42
ap	1.43	.68	.74	3.10	.71	1.36	.88	1.23
ns	.54	0	0	0	0	0	0	0
X_{Fe}	.45	.48	.42	.37	.34	.26	.29	.26
FeNi	.41	.27	.47	.57	.30	.17	.19	.04
FeS	.12	.05	.07	.08	.28	.51	.13	.10

of these UOCs show relatively narrow compositional ranges, with a few exceptions, on the SiO_2-oxides variation diagrams, with average compositions: SiO_2=36–39 wt%, FeO=25–38 wt%, MgO=18–28 wt%, Al_2O_3=2–3 wt%, CaO=0.8–1.2 wt%, Na_2O=0.6–1.2 wt% and K_2O=0.1–0.35 wt%. Although the chondrule rims of Sharps and Chainpur have similar compositional ranges to those of the matrices, the rims of ALH-77214 and Mezö-Madaras are distinguishable from the matrices; they have higher SiO_2, CaO and Na_2O contents, and lower FeO and MgO contents.

The matrix of Tieschitz has characteristically high SiO_2 content (45 wt% in average), similar to that of Semarkona matrix (47 wt%), relatively low FeO (22 wt%), and high alkalis (Na_2O=5 wt%) and Al_2O_3 (8 wt%) contents (Table 3). These analyses include those of the matrix corresponding to the 'white matrix' of CHRISTOPHE MICHEL-LÉVY (1976). On the other hand, the rims have higher FeO and MgO, and lower SiO_2, Al_2O_3, CaO and Na_2O contents than the matrix (Table 3). Compared with the average matrix composition of Semarkona, that of Tieschitz is higher in Al_2O_3, CaO and Na_2O,

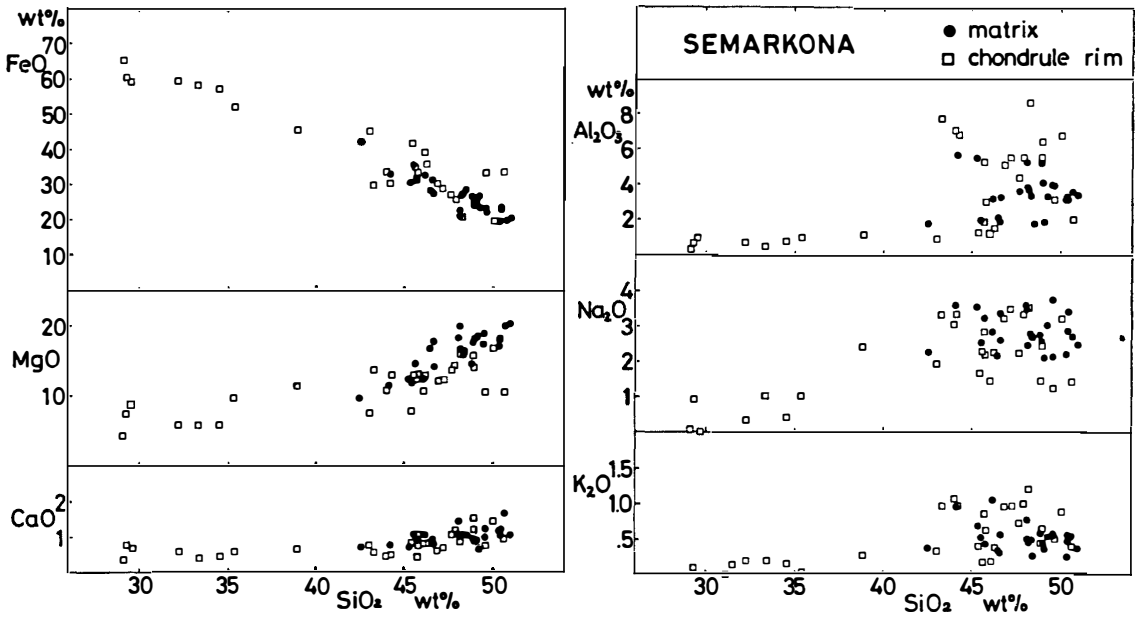

Fig. 8. SiO_2-oxides variation diagrams of matrix and chondrule rim analyses of the Semarkona chondrite. In Semarkona, chondrule rims show wider variations in chemical composition than matrix.

and lower in FeO and MgO (Table 3), and is characterized by high pl and substantial ne in their norms.

Distinctive features of the matrix of ALH-77216 are its high SiO_2 content (40–50 wt%), high normative hy and pl and low normative ol (Table 3). The matrix has ranges of MgO content from 18 to 28 wt% and FeO content from 14 to 26 wt%, which are similar those for mean composition of whole rock silicate portion of L-group chondrites (MASON, 1965), but has higher Al_2O_3, Na_2O and K_2O contents than those of whole rock silicate portion. The matrix has the lowest FeO contents among those reported by HUSS *et al.* (1981) for the matrices of the unequilibrated L chondrites.

4.2. Ternary diagrams

Although the matrices and rims are variable in composition, the variations usually have some common features. Ternary diagrams, Si-(Mg+Fe)-Al, Si-Mg-Fe, Al-Na-K, and Al-(Na+K)-Ca are illustrated in Figs. 9a–9d.

4.2.1. (Mg+Fe)-Al-Si diagram

The (Mg+Fe)-Al-Si diagram was used to characterize the chemical features of the matrices of UOCs by IKEDA *et al.* (1981). As shown by IKEDA *et al.* (1981), matrices and rims of most samples fall along (or slightly across) the olivine-albite tie-line (Fig. 9a). However, Semarkona is plotted mainly in the pyroxene-olivine-albite region.

4.2.2 Si-Mg-Fe diagram

Similar diagrams have been already used by many investigators (*e.g.*, MCSWEEN and RICHARDSON, 1977; ALLEN *et al.*, 1980; IKEDA *et al.*, 1981; SCOTT *et al.*, 1982). Although the chemical variations in matrices and rims are widely scattered in general, some trends are clearly observed on the diagrams (Fig. 9b). Especially, the trends in the matrices and rims of Krymka and Semarkona vary in FeO/(FeO+MgO) mole ratio at nearly constant Mg/Si ratio. In other samples, the variations on the diagrams

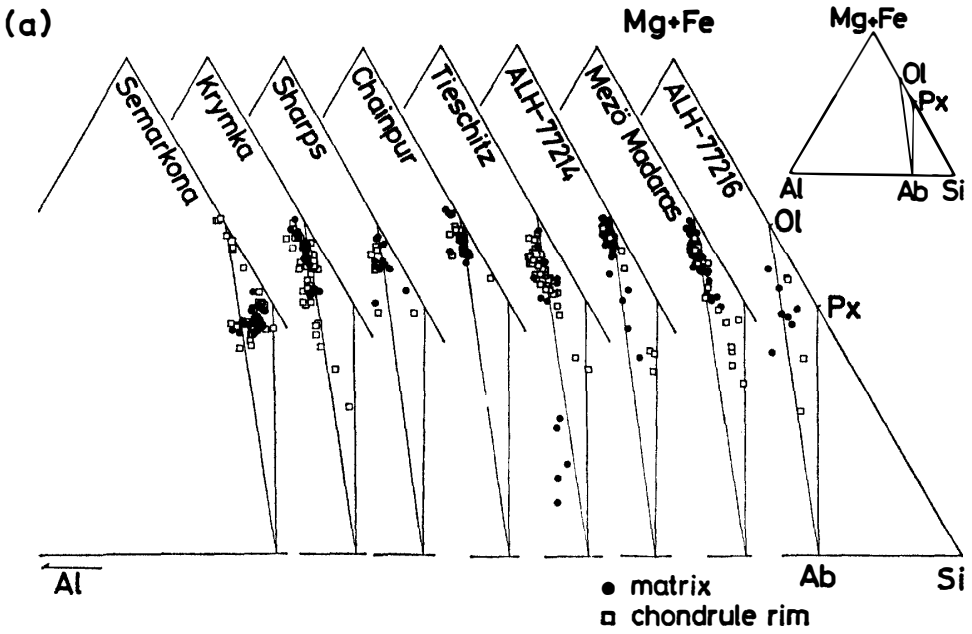

Fig. 9a. The matrix and chondrule rim compositions projected on the ternary plane (Mg+Fe)-Al-Si (atomic percents). All matrices and rims except for those of Semarkona nearly lie along the Ol-Ab tie line. Ol, Px and Ab stand for olivine, pyroxene and albite, respectively.

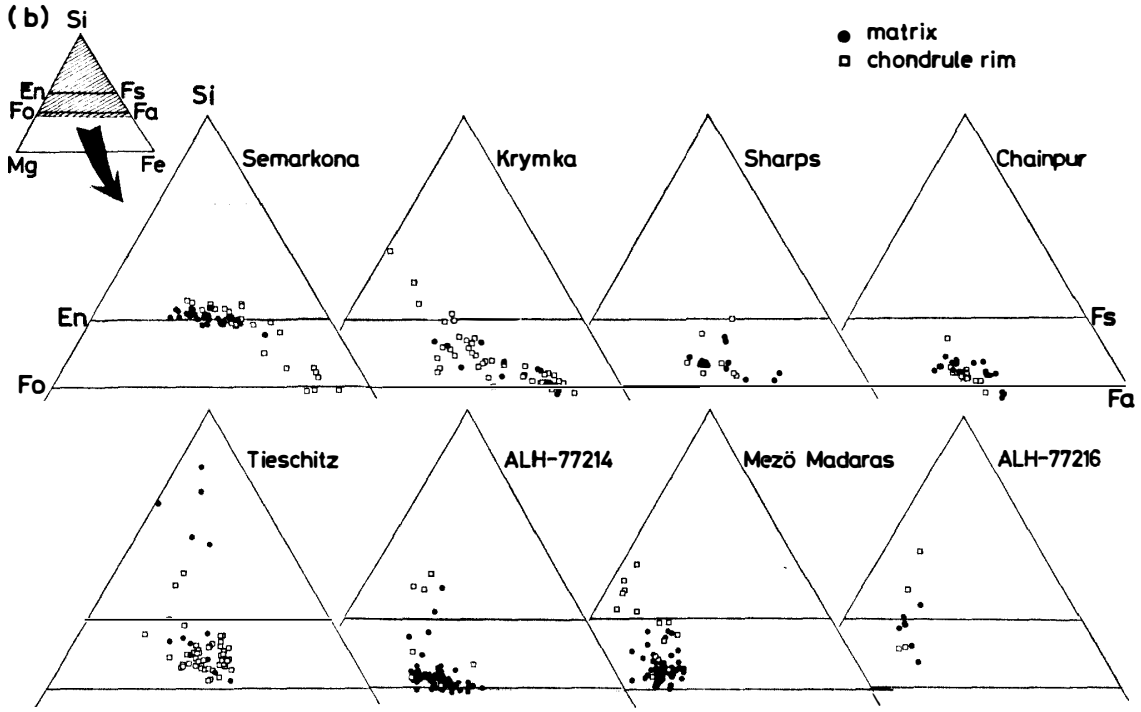

Fig. 9b. The matrix and chondrule rim compositions projected on the ternary plane Si-Mg-Fe (atomic percents). Especially, rim analyses of Semarkona and Krymka show wide variations in Mg/Fe ratio. Fo, Fa, En and Fs stand for forsterite, fayalite, enstatite and ferrosilite, respectively.

are characterized by variable Mg/Si ratios in narrow ranges of Fe/(Mg+Fe) ratios and are located in the more magnesian part near the Si-Mg side line on the diagrams compared with Semarkona and Krymka. These features might be due to increasing degree of equilibration between the iron-rich matrices and rims and the magnesian chondrules, as discussed by HUSS *et al.* (1981).

4.2.3. Al-Na-K diagram

As shown by IKEDA *et al.* (1981), the matrices and rims of these UOCs fall nearly parallel to the Al-Na join (Fig. 9c). The Na/Al ratios are widely variable, ranging from 0 to about 4. Although the matrices and rims are plotted generally across the Ab-Kf tie line, those of Krymka are plotted in Al-rich area above the Ab-Kf tie line. In contrast to Krymka, the matrices and rims of Semarkona are plotted mainly in Na-rich region below the Ab-Kf tie line. However, Semarkona partly includes matrices and rims plotted in Al-rich area of the diagram, showing a characteristically wide variation of Na/Al ratios.

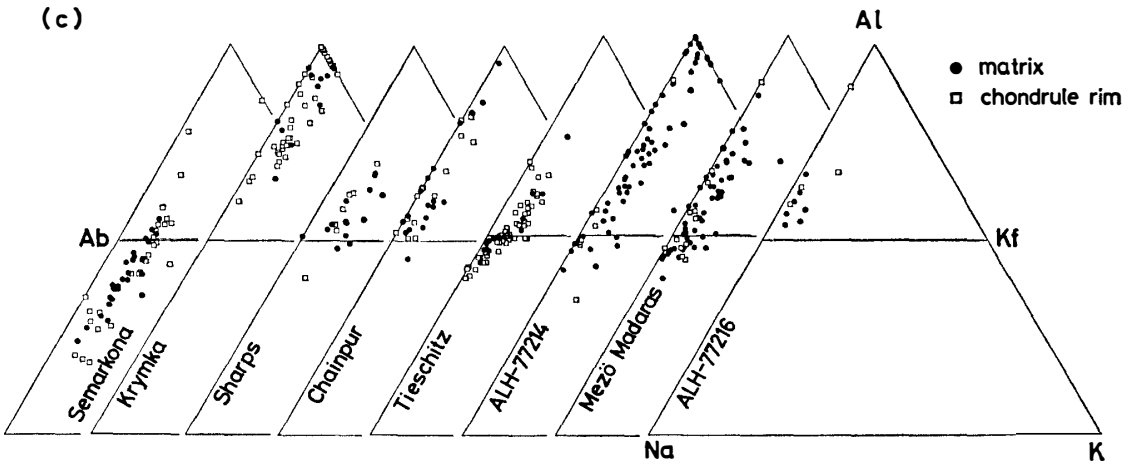

Fig. 9c. The matrix and chondrule rim compositions projected on the ternary plane Al-Na-K (atomic percents). Matrices and chondrule rims of all samples fall nearly parallel to the Al-Na join. Ab and Kf stand for albite and K-feldspar, respectively.

4.2.4. Al-(Na+K)-Ca diagram

Although the compositions are widely scattered and continuous on the diagrams, they have certain characteristics (Fig. 9d). For example, the matrices of Krymka and ALH-77214 are plotted mainly above the Ab-Ca phases tie line, showing a wide range of the (Na+K)/Al ratio. Some of them are plotted above the Ab-An tie line, showing a deficency of the Na content with respect to Al and the presence of normative corundum in the matrices of these samples. However, the rims of these UOCs are plotted mainly on the Ca-richer side than the matrices in nearly the same range of (Na+K)/Al ratios. On the other hand, the matrices and rims of Semarkona are plotted below the Ab-An tie line, furthermore, most of them are plotted below the Ab-Ca phases tie line, showing an excess of the Na content with respect to Al and the presence of small amounts of sodium metasilicate (ns) in their norms. Some of the matrices and rims of Tieschitz also have small amounts of normative ns.

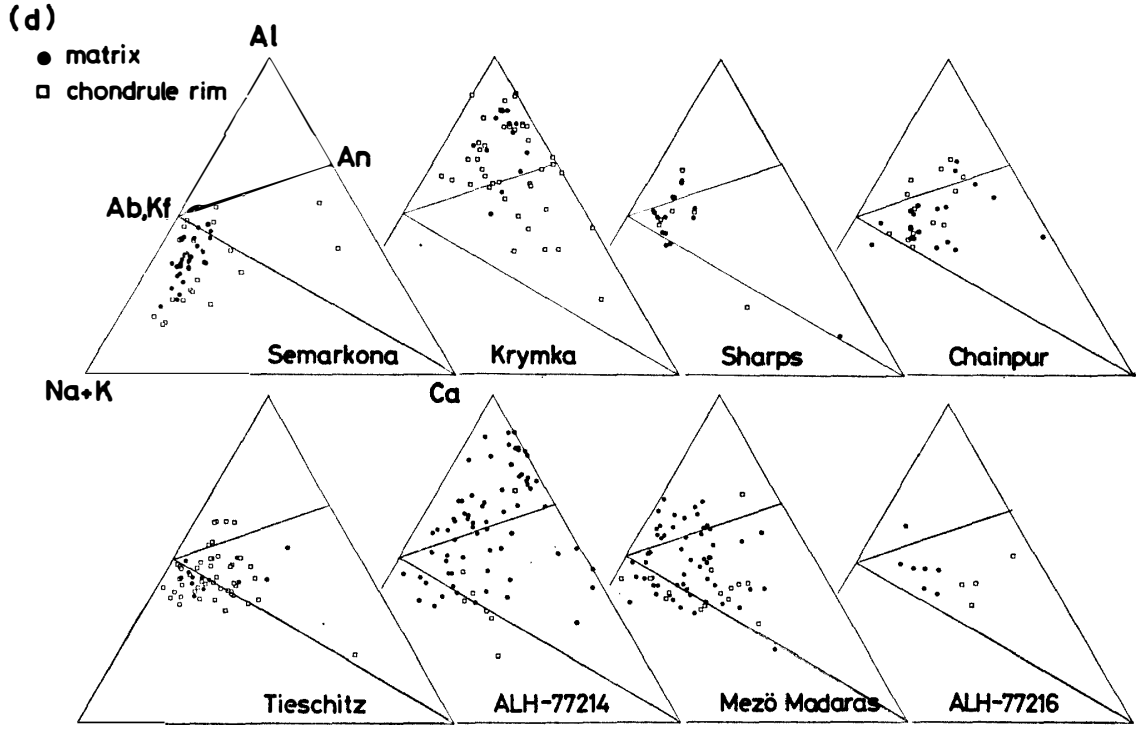

Fig. 9d. The matrix and chondrule rim compositions projected on the ternary plane Al-(Na+K)-Ca (atomic percents). Ab, Kf and An stand for albite, K-feldspar and anorthite, respectively.

5. Discussion

5.1. Compositional relationships among chondrules, matrix and chondrule rims of Semarkona chondrite

As shown in Fig. 10a, the present study has revealed that matrix and chondrule rims of Semarkona are characterized by their lower Mg/Si ratios (0.2–0.6), and qualitatively comparable variability of Al/Si ratio to chondrules, ranging from 0.01 to 0.21. Chondrule rims of Semarkona have a wider compositional range in this diagram than matrix. It is worth noting that some analyses of chondrule rims are plotted near the origin of the diagram which are characterized by the lowest Al/Si (0.01–0.045) and Mg/Si (0.2–0.45) ratios. Especially, these low Mg/Si- and Al/Si-chondrule rims appear to be located on the lowerside extension of the trend defined by chondrules. On the other hand, matrices and chondrule rims of Semarkona are also characterized by their low Ca/Si ratios, ranging from 0.01 to 0.03 (Fig. 10b). Several chondrule rim analyses of Semarkona also have a different compositional range from those of matrix in the Ca/Si-Al/Si diagram. They are characterized by low Al/Si ratios (0.01–0.45) and low Ca/Si ratios (0.01–0.028), and plotted near the origin of the diagram. They are apparently situated on the lowerside extension of the trend defined by chondrules in the Ca/Si-Al/Si diagram. From these diagrams, some analyses of chondrule rims, which are characterized by the lowest Mg/Si, Al/Si and Ca/Si ratios, lie approximately on the extension of the trend of variation defined by chondrules. Here, they are defined as COMPONENT X. COMPONENT X has the lowest Mg/Si (0.2–0.45), Al/Si

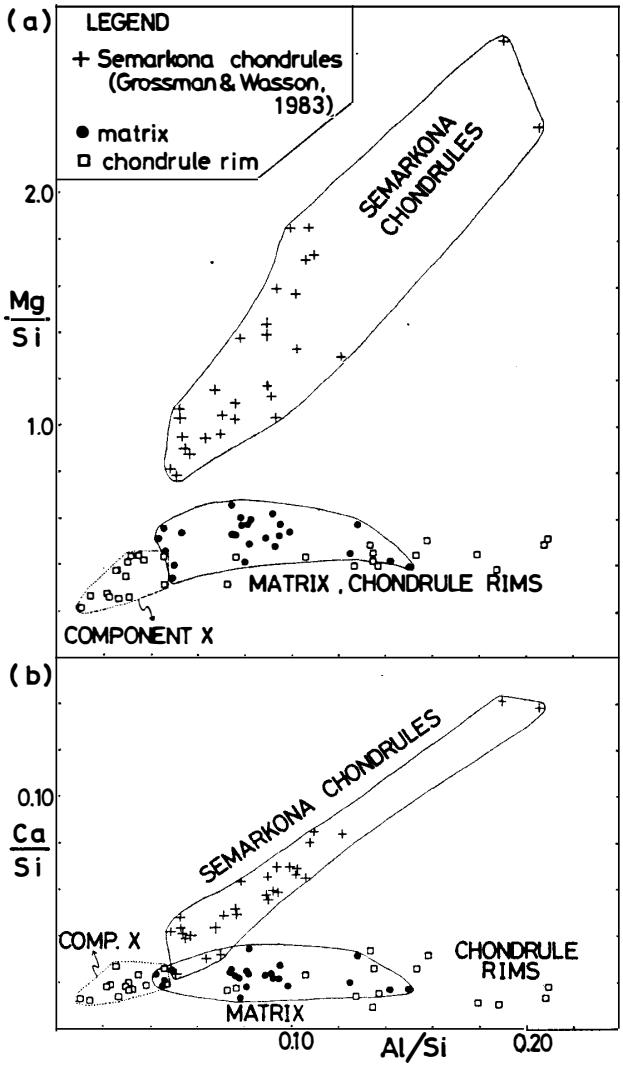

Fig. 10. Molar Mg/Si vs. Al/Si ratios (a) and Ca/Si vs. Al/Si ratios (b) of chondrules, matrices and chondrule rims in Semarkona. Data source of Semarkona chondrules is GROSSMAN *and* WASSON *(1983). The compositional areas of COMPONENT X are also shown in dotted curves (see text for explanation).*

(0.01–0.045) and Ca/Si (0.01–0.028) ratios. Average composition of COMPONENT X is listed in Table 4.

As shown in Figs. 10a and 10b, COMPONENT X is located nearly on the non-refractory-side extension of the compositional trends defined by chondrules, and COMPONENT X may be one of the non-refractory components. Recently, GROSSMAN and WASSON (1983) have published bulk chemical compositions of 30 chondrules from Semarkona, by instrumental neutron activation analysis. They have found that chondrules of Semarkona show refractory element trends similar to those defined by the bulk compositions of ordinary and enstatite chondrites (KERRIDGE, 1979; LARIMER, 1979). They suggested that there are two major chondrule precursor components: a refractory, olivine-rich, FeO-free one and a non-refractory, SiO_2-, FeO-rich one. They

Table 4. Comparison of average composition of COMPONENT X in Semarkona, recalculated to total 100%, on a metallic Ni-Fe- and troilite-free basis (the number of analytical areas averaged N=14), with the non-refractory component of GROSSMAN and WASSON (1983).

	COMPONENT X	Non-refractory component of GROSSMAN and WASSON (1983)
SiO_2	38.5	51.2
TiO_2	.05	
Al_2O_3	1.00	0
Cr_2O_3	.24	.87
FeO	49.1	33.7
MnO	.13	
MgO	8.65	14.3
CaO	.67	0
Ma_2O	1.22	
K_2O	.20	
P_2O_5	.06	

have considered that chondrules would be essentially mixtures of these two components. For comparison, chemical composition of the non-refractory component proposed by GROSSMAN and WASSON (1983) is also presented in Table 4. Although COMPONENT X is more enriched in FeO compared with their non-refractory component, there is a possibility that the compositional trends of the Semarkona chondrules may be explained by the variable mixing ratios of COMPONENT X and the refractory component.

Furthermore, matrix and chondrule rim of Semarkona may be represented roughly by mixtures of COMPONENT X and an Al-enriched component. The Al-enriched component is characterized by high Al/Si ratios and low Ca/Si and Ca/Al ratios. COMPONENT X may be an Al-depleted component of matrix and chondrule rims of Semarkona. Compositional variations of matrix and chondrule rims observed in the Mg/Si-Al/Si and Ca/Si-Al/Si diagrams may be explained by the variable mixing ratios of the Al-depleted COMPONENT X and the Al-enriched component.

In conclusion, it is suggested that Semarkona chondrules and the matrix and rim materials have one common non-refractory component such as COMPONENT X. It has an important role as a linkage among the chondrule precursors, matrices and chondrule rim materials for the genesis of chondritic materials of UOCs.

5.2. Compositional and textural differences between matrix and chondrule rims

As already shown in Section 3, chondrule rims have resemblances in textural features to matrices in each sample. They are composed of the similar fine-grained materials to those in matrices and show similar textures. However, in some respects, textures of rims are different from those of matrices. First, chondrule rims often appear less porous than matrices in Semarkona and Tieschitz, as reported by ASHWORTH (1977) for dark rims of Chainpur. Second, chondrule rims often show remarkable layered structures (Section 3.2.2) (ALLEN *et al.*, 1980; ASHWORTH, 1977). These marked features suggest that rim materials seem to have been deposited directly on the surface of chondrules before accretion of matrix materials (ALLEN *et al.*, 1980; KING and KING, 1981).

Although compositional ranges of chondrule rims considerably overlap those of matrices in each sample, as shown in Section 4, chondrule rims do not always show the same ranges as matrices (*e.g.*, Fig. 8; Figs. 9a–9d). For example, the chondrule rims in Semarkona show wider variabilities in chemical composition compared with the matrix (Figs. 8, 9b, 10a and 10b). Furthermore, in Semarkona there are chondrule rims enriched in COMPONENT X, which might have been the non-refractory component of the Semarkona chondrule precursors. From these facts, it is shown that chondrule rims often have significantly different compositions from the matrix in each sample. Moreover, from comparisons of matrices and chondrule rim analyses with representative analyses of bulk chondrites (compiled by DODD, 1981), using Si-normalized atomic ratios of the refractory lithophile elements (*i.e.*, Mg/Si, Al/Si and Ca/Si) for average compositions of matrices and chondrule rims (Figs. 11a and 11b), we can easily find

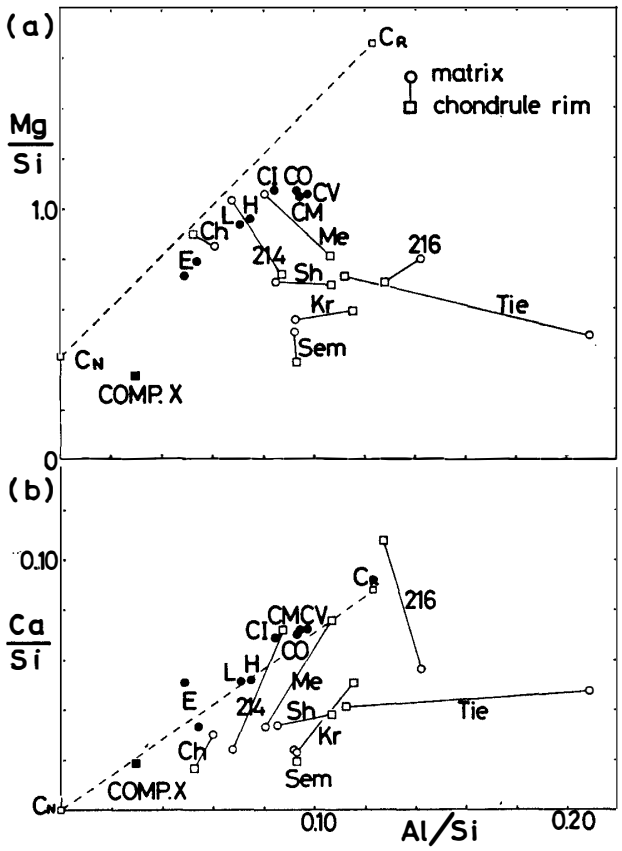

Fig. 11. Molar Mg/Si vs. Al/Si ratios (a) and Ca/Si vs. Al/Si ratios (b) of matrix and chondrule rims from chondrite samples studied (in average). Solid line connects average matrix analysis with average rim analysis for each sample. Solid circles represent average bulk compositions of carbonaceous (CI, CM, CO, CV) and ordinary (H, L) chondrites and representative two of enstatite chondrites, compiled by DODD (1981). Solid square represents average composition of COMPONENT X (see text for explanation). Dashed lines, connecting C_N with C_R, are "chondrule mixing lines" obtained by GROSSMAN and WASSON (1983). Symbols: Sem=Semarkona, Kr= Krymka, Sh= Sharps, Ch= Chainpur, Tie= Tieschitz, Me= Mezö-Madaras, 214= ALH-77214, 216= ALH-77216, C_R and C_N= the refractory and non-refractory components of GROSSMAN and WASSON (1983), COMP.X= COMPONENT X in this study.

that, in most samples, the chondrule rims are plotted in different positions of the diagrams from the matrices. These differences between matrices and rims cannot be neglected, because the differences are comparable to the compositional variations observed among E, O and C chondrites due to fractionation of refractory lithophile elements (LARIMER and ANDERS, 1970; KERRIDGE, 1979; LARIMER, 1979).

In conclusion, it is suggested that chondrule rims may be distinguished from matrices strictly on the basis of textural and compositional differences. Of course, we probably need more detailed information on chemical and isotopic compositions to draw definite conclusions. However, it is important to note the textural and compositional differences between matrices and chondrule rims in UOCs.

Acknowledgments

The author is grateful to Prof. I. KUSHIRO and Dr. H. NAGAHARA of the University of Tokyo for their kind suggestions, discussions, encouragement during this work and critical reading of the manuscript. He also thanks Drs. K. YOKOYAMA and Y. SAITO of the National Science Museum for valuable discussions and permitting him to use the scanning electron microscope, JEOL-T200. He is grateful to Drs. T. NAGATA and K. YANAI of the National Institute of Polar Research and Dr. B. MASON of the Smithsonian Institution for providing and loaning polished thin sections and meteorite samples studied here.

References

ALLEN, J. S., NOZETTE, S. and WILKENING, L. L. (1980): A study of chondrule rims and chondrule irradiation records in unequilibrated ordinary chondrites. Geochim. Cosmochim. Acta, **44**, 1161–1175.

ANDERS, E. (1964): Origin, age, and composition of meteorites. Space Sci. Rev., **3**, 583–714.

ASHWORTH, J. R. (1977): Matrix textures in unequilibrated ordinary chondrites. Earth Planet. Sci. Lett., **35**, 25–34.

CHRISTOPHE MICHEL-LÉVY, M. (1976): La matrice noire et blanche de la chondrite de Tieschitz (H3). Earth Planet. Sci. Lett., **30**, 143–150.

DODD, R. T. (1981): Meteorites; A petrologic-Chemical Synthesis. Cambridge, Cambridge Univ. Press, 368 p.

DODD, R. T. and VAN SCHMUS, W. R. (1971): Dark zoned chondrules. Chem. Erde, **30**, 59–69.

GROSSMAN, J. N. and WASSON, J. T. (1983): Refractory precursor components of Semarkona chondrules and the fractionation of refractory elements among chondrites. Geochim. Cosmochim. Acta, **47**, 759–771.

GROSSMAN, L. and LARIMER, J. W. (1974): Early chemical history of the solar system. Rev. Geophys. Space Phys., **12**, 71–101.

HUSS, G. R., KEIL, K. and TAYLOR, G. J. (1981): The matrices of unequiliblated ordinary chondrites; Implications for the origin and history of chondrites. Geochim. Cosmochim. Acta, **45**, 33–51.

IKEDA, Y., KIMURA, M., MORI, H. and TAKEDA, H. (1981): Chemical compositions of matrices of unequiliblated ordinary chondrites. Mem. Natl Inst. Polar Res., Spec. Issue, **20**, 124–144.

KEIL, K. (1969): Meteorite composition. Handbook of Geochemistory, Vol. 1, ed. by K. H. WEDEPOHL. Berlin, Springer, 78–115.

KERRIDGE, J. F. (1979): Fractionation of refractory lithophile elements among chondritic meteorites. Proc. Lunar Planet. Sci. Conf., 10th, 989–996.

KING, T. V. V. and KING, E. A. (1981): Accretionary dark rims in unequilibrated chondrites. Icarus,

48, 460–472.

LARIMER, J. W. (1979): The condensation and fractionation of refractory lithophile elements. Icarus, **40**, 446–454.

LARIMER, J. W. and ANDERS, E. (1967): Chemical fractionations in meteorites—II. Abundance patterns and their interpretation. Geochim. Cosmochim. Acta, **31**, 1239–1270.

LARIMER, J. W. and ANDERS, E. (1970): Chemical fractionations in metorites—III. Major element fractionations in chondrites. Geochim. Cosmochim. Acta, **34**, 367–387.

LUX, G., KEIL, K. and TAYLOR, G. J. (1980): Metamorphism of the H-group chondrites; Implications from compositional and textural trends in chondrules. Geochim. Cosmochim. Acta, **46**, 557–563.

MASON, B. (1965): The chemical composition of olivine-bronzite and olivine-hypersthene chondrites. Am. Mus. Novit., **2223**, 1–38.

MATSUNAMI, S. (1984): Petrographical studies on matrix and chondrule-rim of unequilibrated ordinary chondrites. Master's thesis, Univ. of Tokyo, 165 p.

MCSWEEN, H. Y. and RICHARDSON, S. M. (1977): The composition of carbonaceous chondrite matrix. Geochim. Cosmochim. Acta, **41**, 1145–1161.

NAGAHARA, H. (1984): Matrices of type 3 ordinary chondrites—Primitive nebular records. submitted to Geochim. Cosmochim. Acta.

SCOTT, E. R. D., TAYLOR, G. L. and KEIL, K. (1982): Origins of ordinary and carbonaceous chondrites and their compositions (abstract). Lunar and Planetary Science XIII. Houston, Lunar Planet. Inst., 704–705.

WOOD, J. A. (1963): On the origin of chondrules and chondrites. Icarus, **2**, 152–180.

(Received July 12, 1984; Revised manuscript received September 25, 1984)

Appendix. Representative analyses of matrices and chondrule rims in the Semarkona (LL3), Krymka (L3), Sharps (H3), Chainpur (LL3), Tieschitz (H3), Mazö-Madaras (L3), ALH-77214 (L3) and ALH-77216 (L3) chondrites. Analytical method is shown in text; —: not detected.

	Semarkona matrix										Semarkona chondrule rim				
SiO_2	32.0	40.9	37.6	42.2	41.3	38.2	35.0	41.8	37.5	36.0	34.0	42.0	47.2	42.4	40.3
TiO_2	.06	.07	.20	.20	.02	.02	.01	—	—	.14	—	.19	—	.13	.30
Al_2O_3	4.08	2.64	2.51	2.80	3.12	3.07	3.74	1.52	1.47	4.34	.89	1.63	5.36	7.58	3.64
Cr_2O_3	.14	.52	.34	.39	.42	.31	.16	.19	.57	.21	.07	.35	.87	.59	.42
FeO	23.8	18.4	17.9	16.8	23.0	17.5	19.0	24.6	25.6	24.5	50.0	32.4	24.1	18.2	22.9
MnO	.22	.28	.28	.18	.06	.34	.38	.44	.19	.27	.20	—	.07	.12	.38
MgO	8.32	14.3	14.1	16.7	14.3	13.4	10.4	14.1	11.4	9.87	9.16	11.9	15.4	14.0	11.6
CaO	.51	.86	.46	.85	.88	.75	.64	.91	.72	.57	.51	1.01	1.48	.71	.87
Na_2O	2.61	2.74	2.30	2.04	2.08	2.86	1.98	2.32	2.71	2.80	.99	2.07	1.36	3.06	2.74
K_2O	.68	.44	.40	.61	.39	.43	.42	.23	.24	.52	.01	.15	.43	1.05	.61
P_2O_5	—	—	.13	—	—	.17	—	—	—	.16	—	.17	.19	—	.76
FeNi	.26	.50	.32	.65	.53	.40	.32	.50	.36	.22	.33	.87	.88	.64	.32
FeS	.22	.39	.35	.38	.44	.27	.17	.48	.41	.18	.26	.47	.80	.32	.31
Total	72.90	82.04	76.89	83.80	86.54	77.72	72.22	87.09	81.17	79.78	96.42	93.21	98.14	88.80	85.15

					Krymka matrix							Krymka chondrule rim		
SiO_2	42.3	29.6	41.7	40.8	31.5	32.4	32.1	30.5	34.7	27.4	39.9	46.2	36.6	30.5
TiO_2	.15	.07	.12	—	—	—	.09	.17	.21	.04	.15	.20	.11	—
Al_2O_3	4.58	.64	4.86	6.53	2.01	2.28	1.80	1.73	2.75	1.08	3.67	6.97	4.64	1.73
Cr_2O_3	.22	.39	.32	.08	.32	.32	.43	.11	.26	.28	.25	.16	.29	.28
FeO	27.4	60.8	25.4	30.8	47.4	47.5	42.5	53.1	40.6	55.3	23.2	9.28	38.6	53.9
MnO	.34	—	.39	.13	.34	.74	.23	.72	.47	.32	.16	.17	.24	.48
MgO	10.9	7.43	10.9	10.1	8.71	9.03	14.0	9.32	12.5	8.45	20.1	16.2	16.3	8.84
CaO	.53	.72	.59	.39	.76	.98	.94	.23	.39	.15	.90	9.34	.67	.34
Na_2O	2.91	.91	3.07	2.79	.06	.13	.45	.26	.10	—	.10	.99	1.35	.11
K_2O	.86	.09	.85	.96	.08	.18	.18	.04	.03	—	.15	.62	.12	—
P_2O_5	—	.26	—	.08	.22	.09	—	—	—	—	—	.70	—	—
FeNi	.49	.33	.42	.27	.42	.50	.76	.45	1.11	.19	1.93	1.21	.71	.07
FeS	.40	.49	.30	.17	.04	.04	.06	.10	.04	.05	.06	.03	.27	.06
Total	91.08	101.73	88.92	93.10	91.86	94.19	93.54	96.73	93.16	93.26	90.57	92.07	99.90	96.31

Appendix (continued).

												Sharps matrix		
SiO_2	30.9	38.1	42.7	31.5	36.1	39.6	31.7	37.5	35.8	37.8	30.8	33.1	31.7	34.5
TiO_2	.18	.26	.04	—	.24	.26	.01	.23	.15	.16	.04	.08	.15	.05
Al_2O_3	1.78	6.40	6.18	1.66	5.52	5.09	1.26	4.28	4.09	3.29	1.19	.76	3.28	2.82
Cr_2O_3	.55	.09	.43	.25	.13	.49	.17	.45	.31	.38	.08	.14	.27	.26
FeO	52.4	28.7	21.8	52.5	29.8	26.5	46.6	27.1	31.7	30.3	49.3	49.6	27.6	29.6
MnO	.13	.53	.35	.69	.54	.41	.44	—	.52	.29	.39	.85	.56	.78
MgO	9.77	15.2	16.8	7.58	15.2	20.1	11.0	18.2	15.4	19.0	7.78	10.3	17.8	18.8
CaO	.30	1.86	2.27	.41	1.39	1.09	1.02	2.18	.61	.86	.76	.30	.53	1.00
Na_2O	.24	1.21	1.19	.08	1.21	.20	.07	.76	.71	—	—	.27	.73	.76
K_2O	.08	.21	.33	—	.44	.11	.12	.26	.23	.12	—	.06	.35	.36
P_2O_5	—	—	—	.08	—	.19	—	.30	.08	.16	—	.06	.46	.76
FeNi	.61	.09	.05	.04	.03	.11	.03	.06	.03	.12	.04	.02	.02	.01
FeS	.60	1.39	1.57	.73	.64	1.45	.85	1.02	1.09	1.04	.75	.38	.12	.37
Total	97.54	94.04	93.71	95.52	91.24	95.60	93.27	92.34	90.72	93.52	91.13	95.92	83.57	90.07
			Sharps chondrule rim				Chainpur matrix						Chainpur chondrule rim	
SiO_2	33.9	38.0	36.9	31.4	37.9	42.0	32.0	34.7	33.5	34.4	29.0	34.0	43.1	33.4
TiO_2	.06	.14	.07	.12	—	.21	.12	.33	—	.02	.20	.11	.02	.14
Al_2O_3	2.08	1.17	4.13	1.92	6.50	1.75	1.10	4.14	1.48	2.47	.96	1.16	.71	1.32
Cr_2O_3	.42	.22	.41	.54	.41	.29	.36	.55	.61	.46	.31	.08	.67	.26
FeO	28.9	30.0	28.5	37.1	24.5	29.7	39.7	31.6	26.5	30.0	45.0	39.1	26.8	33.6
MnO	.34	.43	.47	.51	.22	.42	.70	.50	.29	.30	.54	.89	.50	.34
MgO	18.1	13.2	21.9	15.1	15.3	11.4	15.0	21.6	21.8	19.6	15.9	16.7	20.5	19.0
CaO	.37	7.92	.79	.44	1.55	4.19	.42	2.77	.69	.43	.47	.53	.31	.34
Na_2O	.53	.57	1.35	.90	2.48	1.41	.47	.35	.41	1.31	.45	.59	.11	.22
K_2O	.38	.10	.30	.23	.55	.24	.08	.11	—	.09	.09	.05	.05	.03
P_2O_5	—	—	—	—	.10	—	.14	.42	.10	.23	—	—	.26	—
FeNi	.52	.22	.27	—	.60	.41	.09	.06	.16	.16	.09	.12	.36	.14
FeS	.03	.02	.08	.01	.05	.03	.01	.64	.05	.06	.11	.02	.03	.02
Total	85.63	91.99	95.17	88.27	90.16	92.05	90.19	97.77	85.59	89.53	93.12	93.35	93.42	88.81

Appendix (continued).

			Tieschitz matrix						Tieschitz chondrule rim				
SiO_2	34.2	33.5	46.1	43.7	39.5	32.8	35.3	35.7	37.1	33.5	36.2	36.1	33.5
TiO_2	.06	—	.07	.24	.23	.22	.10	.02	.13	.12	.13	.32	.03
Al_2O_3	.95	1.44	11.9	13.1	10.2	2.23	2.52	4.73	2.74	2.54	2.34	4.80	4.24
Cr_2O_3	.44	.32	.09	.15	.16	.36	.38	.18	.33	.26	.28	.17	.24
FeO	32.0	34.5	.42	5.29	8.00	34.0	30.9	24.5	29.0	26.3	29.0	26.7	26.7
MnO	.44	.62	.25	.07	.15	.69	.48	.17	.23	.47	.33	.71	.14
MgO	21.8	19.9	8.66	4.19	7.09	17.6	17.6	13.9	15.3	21.1	19.3	18.4	19.6
CaO	.44	.41	3.17	1.67	2.09	.74	1.37	1.11	1.98	.69	1.22	.35	.53
Na_2O	.53	.79	7.14	8.95	6.60	1.29	1.13	3.18	2.04	2.34	1.05	2.70	2.91
K_2O	—	.09	.45	.34	.19	.12	.25	.22	.19	.05	.31	.49	.15
P_2O_5	.12	—	1.79	.34	.43	.38	.30	—	.95	.19	.32	.57	.37
FeNi	.40	.21	1.03	.13	—	.18	.29	.26	.40	.22	.18	.82	.12
FeS	.06	.02	.36	.01	.02	.02	.02	.04	.01	.02	.03	.04	.03
Total	91.44	91.80	81.43	78.18	74.66	90.63	90.64	84.01	90.40	87.80	90.69	92.17	88.56

	ALH-77214 matrix						ALH-77214 chondrule rim					Mezö-Madaras matrix		
SiO_2	32.7	34.6	31.3	36.2	31.4	33.0	32.5	41.7	50.7	34.6	51.4	39.6	37.9	36.7
TiO_2	.06	.25	.04	.04	.26	.04	.05	.24	.16	.22	.23	.08	.03	.22
Al_2O_3	1.37	3.09	2.16	1.43	.97	1.73	2.03	2.38	4.77	1.55	4.32	3.69	1.73	2.06
Cr_2O_3	.44	.46	.55	.33	.37	.55	.42	.35	.56	.49	.91	1.34	.70	.44
FeO	30.8	29.7	30.9	30.2	41.1	39.7	32.2	22.0	14.1	34.1	11.3	24.2	23.4	26.0
MnO	.32	.34	.54	.75	.71	.57	.28	.34	.65	.51	.46	.35	.75	.49
MgO	25.6	23.1	22.8	23.7	18.4	21.1	24.0	26.1	17.6	16.9	18.7	24.0	28.2	27.8
CaO	.45	.73	1.09	.35	.48	.20	.93	1.66	4.93	2.63	5.14	1.84	.82	.31
Na_2O	.32	.31	.36	.41	.49	.35	.93	1.24	2.93	1.19	2.78	2.51	.60	1.33
K_2O	.07	.31	—	.14	.10	.06	.02	.10	.09	.23	.12	.10	.06	.16
P_2O_5	—	.33	.81	.21	.41	.85	.12	.06	2.57	.64	3.41	.07	.22	—
FeNi	.26	.38	.34	.47	.41	.17	1.04	.31	.15	.47	.31	.31	.55	.35
FeS	.03	.04	.02	.02	.02	.08	.06	.34	.03	.06	.04	.21	.03	.04
Total	92.42	93.64	90.91	94.25	95.12	98.40	94.58	96.82	99.24	93.59	99.12	98.30	94.99	95.90

Appendix (continued).

					Mezö-Madaras chondrule rim					ALH-77216 matrix			
SiO_2	35.4	37.1	35.6	38.2	37.5	38.3	52.0	51.3	56.9	42.3	46.6	46.7	48.3
TiO_2	.17	.22	.17	.03	.02	.05	.22	.33	.37	.24	.14	—	.05
Al_2O_3	2.87	3.27	1.87	1.66	2.67	1.95	5.66	6.75	6.85	4.03	6.25	3.15	5.30
Cr_2O_3	.42	.56	.50	.53	.59	.41	.83	.64	.82	.30	.66	.18	.32
FeO	26.8	26.6	27.1	25.8	28.4	27.1	4.19	2.69	3.52	20.5	15.0	15.7	14.3
MnO	.27	.63	.34	.33	.45	.41	.66	.66	.86	.55	.40	.61	.33
MgO	23.4	26.8	29.9	27.3	25.0	26.7	24.7	22.0	20.1	25.4	25.8	24.3	23.8
CaO	.29	.42	.58	.96	.16	.99	5.14	6.77	5.98	2.98	1.67	1.71	3.13
Na_2O	1.01	1.54	.44	.92	1.82	1.32	1.92	3.15	3.10	1.74	2.75	1.09	2.56
K_2O	.25	.17	—	.08	.33	.19	.09	.11	.21	.42	.22	.11	.29
P_2O_5	.10	.15	.54	.14	.53	.07	—	2.78	—	.70	.32	.16	.04
FeNi	.21	.20	.21	.13	.17	.05	.09	.35	—	.32	.06	.02	.31
FeS	.14	.16	.12	.04	.07	.16	—	.10	.04	.02	.06	.13	.18
Total	91.33	97.82	97.34	96.12	97.71	97.70	95.50	97.63	98.75	99.50	99.93	93.86	98.91

	ALH-77216 chondrule rim		
SiO_2	45.4	45.9	51.3
TiO_2	.04	.09	.39
Al_2O_3	2.31	2.14	6.20
Cr_2O_3	.57	.67	.34
FeO	20.4	19.6	10.5
MnO	.12	.39	.30
MgO	28.7	30.2	19.7
CaO	2.07	1.85	7.04
Na_2O	.51	.15	2.48
K_2O	.26	.01	.17
P_2O_5	—	.03	.38
FeNi	—	.11	—
FeS	.13	.16	.02
Total	100.51	101.30	98.82